Nanotoxicology, November 2012; 6(7):746–756
© 2012 Informa UK, Ltd.
ISSN: 1743-5390 print / 1743-5404 online
DOI: 10.3109/17435390.2011.620717

informa
healthcare

Organ biodistribution, clearance, and genotoxicity of orally administered zinc oxide nanoparticles in mice

Ching-Hao Li[1,*], Chuan-Chou Shen[2,*], Yu-Wen Cheng[3], Shih-Hsuan Huang[1], Chung-Che Wu[2], Chen-Chieh Kao[1], Jiunn-Wang Liao[4] & Jaw-Jou Kang[1]

[1]Institute of Toxicology, College of Medicine, National Taiwan University, Taipei, Taiwan, [2]Department of Geosciences, High-precision Mass Spectrometry and Environment Change Laboratory, National Taiwan University, Taipei, Taiwan, [3]School of Pharmacy, Taipei Medicine University, Taipei, Taiwan and [4]Graduate Institute of Veterinary Pathology, College of Veterinary Medicine, National Chung Hsing University, Taichung, Taiwan

Abstract

Understanding tissue biodistribution and clearance of zinc oxide nanoparticles (ZnO-NPs) is necessary for its risk assessment. Both fed and intraperitoneally injected ZnO-NPs (2.5 g/kg) were absorbed into circulation (within 30 min post-dosing), then biodistributed to the liver, spleen, and kidney. Intraperitoneally injected ZnO-NPs remained in serum for 72 h and could more effectively spread to the heart, lung, and testes, whereas the clearance for fed ZnO-NPs in serum began 6 h after oral administration. Compared with zinc oxide microparticles (ZnO-MPs), ZnO-NPs exhibited much higher absorptivity and tissue biodistribution in fed treatment. A greater fraction of fed ZnO-NPs localised in the liver resulted in transient histopathological lesions. However, superoxide generation and cytotoxicity were showed *in vitro* treatment with ZnO-NPs (above 20 μg/mL). Considering both *in vitro* and *in vivo* data, the ZnO-NPs induced acute liver toxicity which was in compliance with its absorption, biodistribution, and clearance.

Keywords: Zinc oxide, nanoparticles, clearance, absorption, biodistribution

Introduction

The rapid development in nanotechnology has spawned numerous novel products and applications (Riehemann et al. 2009). According to the definition by the International Standards Organization (ISO), nanoscale substances are those substances that have at least one external dimension in the size range below 100 nm. Due to their small size and corresponding large surface area, nanoscale substances usually have unique physical and/or chemical characteristics, which are significantly different from the bulk versions of the same material. Moreover, the propensity of nanoscale substances to get adsorbed, penetrated, and internalised within biological systems may pose an extraordinary hazard to humans (Klaine et al. 2008; Stone & Donaldson, 2006). Many scientific reports have cautioned that nanoscale particles are thought to impose more serious adverse effects on human health than microscale particles (Oberdörster et al. 2005; Nel et al. 2006). In principle, each relevant element, including the intake, biodistribution and accumulation, metabolism and excretion, should be investigated individually and extensively for risk assessment (Maynard et al. 2007).

Zinc oxide (ZnO), one of the most common metal oxides, has been traditionally utilised in paint formulation and ceramic manufacture. Recently, ZnO nanoparticles (ZnO-NPs) have been made and are used in protective sunscreen cosmetics, dental composites, and dermal ointments (Sevinc & Hanley 2010; Cross et al. 2007). ZnO-NPs have a wide range of antibacterial activities towards various microorganisms, which is not possessed by ZnO microparticles (ZnO-MPs). The antibacterial activity of ZnO-NPs was size-dependent and might involve the production of reactive oxygen species (ROS) (Reddy et al. 2007; Raghupathi et al. 2011). Induced oxidative stress, exerted inflammatory responses, and cytotoxic effects were found in ZnO-NPs-exposed human cell systems (Pujalté et al. 2011; Hackenberg et al. 2011). As a well-known photocatalyst, co-treatment of ZnO-NPs and ultraviolet A (UVA) in cancer cell lines significantly generated more ROS and reduced the vitality, when compared with those cells treated with ZnO-NPs or UVA only (Hackenberg et al. 2010). In mast cells, ZnO-NPs could suppress high affinity IgE receptor (FcεRI)-mediated degranulation and histamine releases and play an important role in the prevention of food allergy (Yamaki & Yoshino 2009; Matsumura et al. 2010).

Correspondence: Jaw-Jou Kang, Institute of Toxicology, College of Medicine, National Taiwan University, 1 Jen-Ai Road, Section 1, Taipei 10, Taiwan. Tel: +886 2 23123456 ext. 88603. Fax: +886 2 23410217. E-mail: jjkang@ ntu.edu.tw
*These authors contributed equally to this work.

(Received 22 September 2010; accepted 1 September 2011)

Nutritional zinc supplementation is beneficial for the prevention and treatment of human disease. Symptoms of zinc deficiencies are tastelessness and loss of appetite (Haase et al. 2008); further, overdoses may negatively influence human health: the symptoms, including nausea, vomiting, dizziness, colic, fever, and diarrhoea. Human body only absorbs 20–40% of zinc present in food. To enhance the bioavailability, the additive ZnO available in the food industry has been replaced by ZnO-NPs. However, the toxicological data, especially the unintended toxicity induced by oral ingestion, currently remains undefined. The objectives of this study were to clarify the differences of uptake, tissue biodistribution, *in vitro* cytotoxicity and mutagenicity, *in vivo* genotoxicity, and acute toxicity between ZnO-NPs and ZnO-MPs through oral administration or intraperitoneal injection.

Materials and methods

Nanoparticles

Uncoated, ZnO-NPs were purchased from Top Nano Technology Co., Ltd. (Taipei, Taiwan). ZnO-MPs were chosen for reference control. The NPs morphology, size, and agglomeration were characterised by using transmission electron microscopy (TEM) and dynamic light scattering (DLS) particle size analyser. The ultrastructure of ZnO-NPs and ZnO-MPs are shown in Figure 1. Almost all ZnO-NPs were in thin-slice-shaped particles with a diameter of approximately 50 nm. Agglomerated particles could be seen but the primary particles were dominant. The ZnO-MPs were compacted crystals with at least one external dimension of >100 nm. DLS showed that ZnO-MPs contain primary particles with an intensity-weighted average hydrodynamic diameter of 1226.2 ± 120.4 nm (>91.6%) and with a low percentage of smaller particles. The intensity-weighted average hydrodynamic diameter of ZnO-NPs was 93.35 ± 14.53 nm.

The suspensions of ZnO particles (stock concentration: 50 mg/mL) were prepared using anhydrous dimethyl sulfoxide (DMSO). ZnO-NPs and ZnO-MPs were diluted with sterile water plus 1% hydroxypropyl methyl cellulose (HPMC) or culture medium, then mixed vigorously, sonicated, and then immediately applied to mice or human cells to minimise agglomeration. Finally, the DMSO concentration was less than 1% (*in vivo* study) and less than 5‰ (*in vitro* study).

Animal husbandry

Male Crl:CD-1 (ICR) mice (6-week-old) were obtained from the Animal Center of National Taiwan University (Taipei, Taiwan) and acclimated for 1 week in the housing room under 12 h of light/dark cycle, 23 ± 1°C, and 39~43% relative humidity; water and food were available *ad libitum*. All procedures involving the use of animals were in compliance with *Guide for the Care and Use of Laboratory Animals* (National Academy of Sciences Press, 1996) and approved by the Institutional Animal Care and Use Committee (approval number: NTUIACUC-20090024).

Micronucleus assay

Male ICR mice (N = 5) were administered ZnO-NPs or ZnO-MPs in an identical manner, orally by intragastric gavage at doses of 1.25, 2.5, and 5.0 g/kg body weight (b.w.). The dosing volume was 10 mL/kg b.w. Negative control received the vehicle, and positive control group was given an intraperitoneal injection of 200 mg/kg b.w. cyclophosphamide. Peripheral blood (10–20 μL) was sampled from the tail vein at 24, 48, and 72 h post-dosing, smeared on a glass microscope slide and stained with acridine orange (40 μg/mL). The prepared slides were immediately examined by fluorescence microscopy. The ratio (%) of polychromatic erythrocytes (PCEs) to total erythrocytes and the frequency of micronucleated polychromatic erythrocytes (MNPCEs) (‰) were calculated by counting a total of 1000 erythrocytes or PCEs per animal, respectively.

14 -Day single-dose acute toxicity study

Thirty mice were divided into three groups (five males and five females per group). Mice were fed with vehicle (control

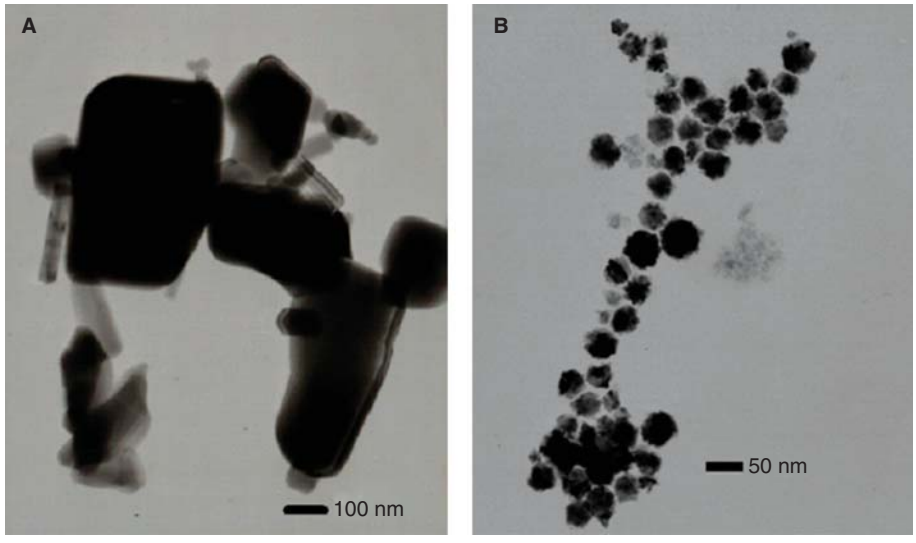

Figure 1. The ultrastructure of ZnO-NPs and ZnO-MPs. Samples were prepared by dropping the ZnO particles suspension on carbon-coated copper transmission electron microscopy (TEM) grids and scanned by using TEM at 120 kV (JEM-2100, JEOL Ltd., Tokyo, Japan). The morphology, size, and agglomeration of ZnO particles were measured manually. (A) ZnO-MPs and (B) ZnO-NPs.

group), 5 g/kg b.w. ZnO-NPs suspension (ZnO-NPs treated group), or 5 g/kg b.w. ZnO-MPs suspension (ZnO-MPs treated group). Dosed mice were conditioned for 14 days. The mortality and clinical behaviour were observed daily. Body weights were recorded twice weekly. At the end of the study (on day 14), the mice were anaesthetised with isoflurane and blood (for serum biochemistry analysis) was collected from the orbital sinus, followed by gross necropsy. Tissue samples (for histopathologic examination) were taken and fixed in 10% neutral buffered formalin.

Serum biochemistry analysis

For serum biochemical analysis, the clotted blood samples were centrifuged at 1500 × *g* for 10 min to obtain serum, and the serum was submitted to biochemical analysis by using an automated analyser (Hitachi Ltd., Tokyo, Japan). The serum biochemistry parameters, including glucose (GLU), blood urea nitrogen (BUN), creatinine (CRE), aspartate aminotransferase (AST; serum glutamic-oxaloacetic transaminase (SGOT)), alanine aminotransferase (ALT; serum glutamic-pyruvic transaminase (SGPT)), alkaline phosphatase, cholesterol, triglycerides, amylase, bilirubin, albumin (ALB), total protein (TP), phosphorus (P), calcium (Ca), sodium (Na), potassium (K), and chlorine (Cl) were analysed.

Histopathology examination

Histologic analysis for toxicity was performed by examining the morphological changes in the organs (heart, liver, spleen, lung, and kidney). The formalin-fixed tissues were trimmed, embedded in paraffin, and sliced into 5-μm thick sections. These biopsy sections were stained with H&E, and examined under light microscope by an experienced pathologist.

Animal treatment of zinc absorption and tissue biodistribution

Male ICR mice (10–12 mice per group) were administered a single-dose of vehicle (control group), 2.5 g/kg b.w. ZnO-NPs suspension (ZnO-NPs treated group), or 2.5 g/kg b.w. ZnO-MPs suspension (ZnO-MPs treated group) through intraperitoneal injection or oral administration. Blood samples (20–30 μL for each time point) were collected at 0.5, 1, 2, 4, 6, 24, 48, and 72 h post-dosing from the orbital sinus by using a glass capillary tube. Before sampling, the mice were anaesthetised with isoflurane. At least three mice were picked from each of the dosed group for blood sampling at the aforementioned time points. Tested mice were sacrificed at 24, 48, and 72 h with an overdose of isoflurane; gross necropsy and tissues sampling (heart, kidney, liver, lung, spleen, testes, and brain) were performed. Both the serum and tissue samples were stored in a freezer at -80°C and analysed for zinc levels.

Inductively coupled plasma-mass spectrometry analysis

The determination of zinc levels in the serum or different tissues/organs were quantified by using inductively coupled plasma-mass spectrometry (ICP-MS) (Element, Finnigan MAT, Germany) analysis. Briefly, the sampled organs were weighed and freeze dried. The freeze-dried sample (100 mg) were digested in a screw cap sample beaker with 2 mL wet-digest solution (75% nitric acid (HNO_3): 70% perchloric acid ($HClO_4$) = 1:1 v/v). The samples were placed on a hot plate overnight at 120°C. After the sample digest was clear, the cover was removed and heating was continued at 80°C until dry. Five percent of HNO_3 was added to dissolve the sample digest residue and the final volume was brought to 5 mL. The resulting solution was then diluted with 5% HNO_3 and the total dilution was made up to 5000 times the original weight of the sample and analysed using ICP-MS. We used calibration standards of 0.1, 1.0, and 10.0 ppb Zn for method validation. All lines were observed from an axial view point of the plasma to increase sensitivity. Three to five replicates per sample were used to obtain the standard deviation (SD) value. All the samples were re-diluted and analysed in duplicates to ensure reproducibility.

Salmonella/microsome reversion assay: Ames test

Salmonella typhimurium histidine auxotrophs, TA98, TA100, TA1537, TA1535, and TA102 were purchased from Molecular Toxicology Inc. (Moltox™, USA). Mutagenicity was determined by incorporation method with the presence and absence of S9 metabolic activation (Cheng et al. 2004; Maron & Ames 1983). A 100 μL of each test bacterial culture (10^9 cells/mL), 2 mL of soft agar (0.6% agar, 0.5% NaCl, 5 mM histidine, and 50 mM biotin, pH 7.4, 40~50°C), 0.5 mL S9 mixture (if necessary), and ZnO-NPs (or ZnO-MPs) were mixed well in a test tube. Subsequently, the sample was immediately poured onto a minimal agar plate (1.5% agar, Vogel–Bonner E medium containing 2% glucose). Plates were incubated in an incubator for 48 h at 37°C in the dark. The revertant colonies were counted macroscopically. A compound was considered positive for mutagenicity only when i) the number of revertants was at least double the spontaneous yield, ii) a statistical significance ($p \leq 0.05$) was found, and iii) a reproducible positive dose–response was present.

Cell culture, cell treatment, and cytotoxicity assay

Human umbilical cords were obtained from the National Taiwan University Hospital, and human umbilical vein endothelial cells (HUVECs) were isolated by enzymatic digestion from a 20-cm long umbilical cord vein segment using 0.1% collagenase as previously described (Liao et al. 2009). Confluent primary cultures within passages three to six were used in the experiments. The hepatocarcinoma cell line, HepG2; the alveolar epithelial cell line, A549; and the mice phagocyte, Raw 264.7 cells were purchased from American Type Culture Collection (ATCC, VA, USA) and maintained in Dulbecco's modified Eagle's medium (DMEM) along with 10% heat-inactivated foetal bovine serum (FBS) in a humidified 5% CO_2 atmosphere at 37°C in an incubator.

Cytotoxicity was evaluated by the reduction of 3-(4,5-dimethyl-2-thiazolyl)-2,5-diphenyl-2H-tetrazolium bromide (MTT) (Liao et al. 2009). The cells were seeded in 48-well plates (1×10^4 cells/well). After 24 h, cells were incubated with ZnO-NPs and ZnO-MPs at the indicated concentrations (0, 5, 10, 20, 50, 100, and 200 μg/mL) for another 24 h. Culture medium with 5‰ DMSO was used as the solvent control. After treatment, MTT was added to each well for a

final concentration of 0.04 mg/mL. After 4 h incubation, the MTT solution was removed and replaced with 200 μL DMSO. Absorbance of the MTT metabolic product, formazan, at 570 nm was measured using an enzyme-linked immunosorbent assay (ELISA) microplate reader. The readings were corrected for background optical density by subtracting the readings from the readings of a blank treatment. The final data were generated from at least three independent assays.

Intracellular superoxide measurement

Superoxide generation was determined using FACSCalibur (BD Biosciences, San Jose, CA, USA). The 8×10^4 HUVECs seeded in a 12-well plate was loaded with 10 μM dihydroethidium (DHE) for superoxide detection. After 10-min staining, cells were exposed to vehicle (5‰ DMSO), ZnO-NPs (10 μg/mL), or ZnO-MPs (10 μg/mL) for the indicated periods (15–180 min) at 37°C in an incubator. The cells were then harvested by trypsinisation, and the fluorescence was measured by flow cytometry. The final data were generated from at least three independent assays.

Statistical analysis

All data were expressed as the mean ± SD from at least three independent experiments ($N \geq 3$). The significance of the difference between the control and each experimental test condition was analysed by Student's *t*-test. Statistically significant differences among groups were determined using one-way analysis of variance (ANOVA). A value of $p < 0.05$ was taken as statistically significant.

Results

No obvious adverse effects were found in ZnO-NPs (or ZnO-MPs) orally treated mice in 14-day single-dose acute toxicity study

The lethal dose, 50% (LD_{50}) of ZnO for rats is >5 g/kg b.w. for single oral ingestion (Yamaki & Yoshino 2009). Thus, the dose designation was set at 5 g/kg b.w. All the mice survived throughout the testing period without exhibiting any abnormalities related to the test compound. In comparison with vehicle control group, ZnO-MPs treated group showed a body weight reduction in both males (days 5 and 10) and females (days 5, 10, and 14); the body weight changes were unobvious in ZnO-NPs treated groups (Supplementary Table I). Decreased wet weights of the spleen, kidney, and liver were observed in ZnO-MPs treated females but not in ZnO-MPs treated males (Supplementary Table II). However, no obvious gross pathological signs were found in the study. All serum biochemistry measures were without any significant alternation except for marginal variations in certain parameters (Supplementary Table III), which suggests that the oral administration of ZnO-NPs or ZnO-MPs in mice did not cause any obvious adverse effects in a 14-day acute toxicity study.

Neither genotoxicity (micronucleus assay) nor mutagenicity (Ames test) were found in ZnO-NPs (or ZnO-MPs) treated system

Reduction in the ratio of PCEs to total erythrocytes (%) and an increase in frequency of MNPCEs (‰) were found in the positive control group. The proportion of PCEs and the frequency of MNPCEs in ZnO-NPs or ZnO-MPs treated (1.25, 2.5, and 5 g/kg b.w.) groups were not statistically different from that of the negative control animals (Supplementary Table IV).

In Ames test, fold-increases in the number of revertants were found in the positive control group. No significant changes of revertants were observed at any concentrations of ZnO-NPs and ZnO-MPs treatments in all five tester strains (TA97, TA98, TA100, TA102, and TA1535) (Supplementary Table V). These data indicated that neither genotoxicity nor mutagenicity existed in ZnO-NPs or ZnO-MPs treated system.

ZnO-NPs have better efficiency in absorption than ZnO-MPs in orally treated mice

Zinc levels in the serum of mice that received a single-dose (2.5 g/kg b.w.) of ZnO-NPs or ZnO-MPs via intraperitoneal injection or oral ingestion were determined by using ICP-MS (Figures 2A and 2B). No significant changes were found in the control group throughout the testing period. In intraperitoneally injected groups, the serum zinc level immediately elevated within 30 min and reached to the peak point at 6 h, then sustained at an equilibratory level over 72 h; however, no significant differences were found in these changes between the ZnO-NPs and ZnO-MPs treated groups (Figure 2A). In the orally ingested mice groups, similar increased serum zinc levels were found within 30 min post-dosing. The maximum absorption occurred at 2 h (18.10 ± 1.63 and 14.63 ± 1.60 μg/g in both ZnO-NPs and ZnO-MPs treated groups, respectively). Within 2–6 h testing period, the mean serum zinc levels of ZnO-NPs treated group were obviously higher than those in the ZnO-MPs treated group. Serum zinc level began to decrease after 6 h and returned to the baseline at 48 h post-dosing (Figure 2B). These data indicated that the ZnO-NPs exhibited better efficiency in absorption than ZnO-MPs for orally ingested treatment but not for intraperitoneally injected treatment.

Intraperitoneal injection of ZnO-NPs (or ZnO-MPs) caused broad tissue biodistribution *in vivo*

Figure 3 represents the tissue biodistribution of zinc in mice that received intraperitoneal injection of 2.5 g/kg b.w. ZnO-NPs or ZnO-MPs. Except the brain (Supplementary Figure 1B), zinc accumulation was found in broad tissues, including the heart, liver, spleen, lung, kidney (Figure 3), and testes (Supplementary Figure 1D). The liver was the major depot where a 2.9- (24 h), 9.4- (48 h), 8.5-fold (72 h) increase in ZnO-NPs treated group and 1.6- (24 h), 3.0- (48 h), 4.5-fold (72 h) increase in ZnO-MPs treated group were observed in comparison with the levels in the control group. In comparison with the potential of biodistribution between ZnO-NPs and ZnO-MPs, the increased zinc levels in the liver, spleen, and lung (Figures 3A–C) of the ZnO-NPs treated group were statistically significant to the ZnO-MPs treated group; but, no significant differences were observed in the kidney, heart (Figures 3D and 3E), and testes (Supplementary Figure 1D).

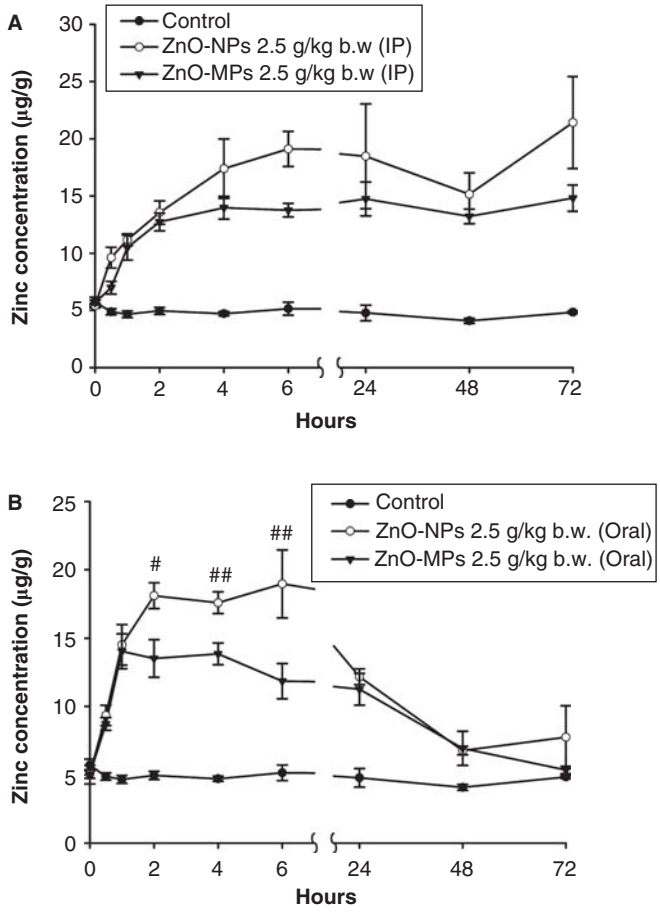

Figure 2. Determination of zinc level in circulation. Mice received single-dose (2.5 g/kg b.w.) of ZnO-NPs (or ZnO-MPs) through intraperitoneal injection (A) or oral ingestion by intragastric gavage (B). Serum was sampled at indicated time point, processed, and the zinc level was analysed by ICP-MS as described in "Materials and Methods section. (A) Serum zinc level immediately elevated in 30 min, and sustained in equilibratory level over 72 h in both ZnO-NPs and ZnO-MPs treated groups. No significant differences were found between ZnO-NPs and ZnO-MPs. (B) Increased serum zinc was found by 30 min post-gavage, and began to decrease after 6 h. Within 2–6 h testing period, mean serum zinc levels of ZnO-NPs treatment were higher than ZnO-MPs treatment. $^{\#}p < 0.05$, and $^{\#\#}p < 0.01$, indicate a significant difference with the ZnO-MPs treated group ($N \geq 3$). b.w.: body weight; ICP-MS: inductively coupled plasma-mass spectrometry; ZnO-MPs: zinc oxide microparticles; ZnO-NPs: zinc oxide nanoparticles.

ZnO-NPs have better efficiency in liver, spleen, and kidney biodistribution than ZnO-MPs in orally treated mice

Tissue biodistribution of zinc in orally treated mice are presented in Figure 4. No changes in the zinc level was observed in the lung, heart (Figures 4C and 4E), brain, and testes (Supplementary Figures 1A and 1C) among the control group, ZnO-NPs treated group, and ZnO-MPs treated group, suggesting that the fed ZnO-NPs and ZnO-MPs were not biodistributed to these organs. But, in the liver, spleen, and kidney (Figures 4A, 4B, and 4D), an elevation in zinc level was found for over 24–72 h post-dosing. In these organs, the detected zinc level increased more obviously in the ZnO-NPs treated mice than in the ZnO-MPs treated group, suggesting that ZnO-NPs treatment cause a more efficient tissue biodistribution.

Absorption and tissue biodistribution of ZnO-NPs and ZnO-MPs varied based on particle size

Solubility data of ZnO-NPs and ZnO-MPs in aqueous solution are summarised in Table I. Under neutral condition (pH 7.0–8.5), the measured zinc ions in tested samples approximated to the ZnO reference solubility (1.6 μg/mL). However, dissociated zinc ions were obviously elevated in an acid condition (pH 2.0; to mimic the gastric/digestive environment), where the ZnO could react to $ZnCl_2$ (reference solubility of 4.32 g/mL at 25°C). The degree of zinc ion release was not significantly different between ZnO-NPs and ZnO-MPs suggesting that the observed changes in absorption and tissues biodistribution in this study resulted from particle size.

ZnO-NPs caused cytotoxic and histopathological lesions in orally treated mice

In the serum biochemistry analysis, the activities of AST, also called SGOT, ALT, also called SGPT, lactate dehydrogenase (LDH) (Figures 5A–C); and the levels of Mg^{2+} and phosphorus (data not shown) were increased in ZnO-NPs and ZnO-MPs orally treated mice groups. However, the changes of these biomarkers were not significantly different between the two treated groups. No significant changes were found for other parameters examined (data not shown). During examination, except that of the liver, no significant histopathological lesions were noted in the sampled organs

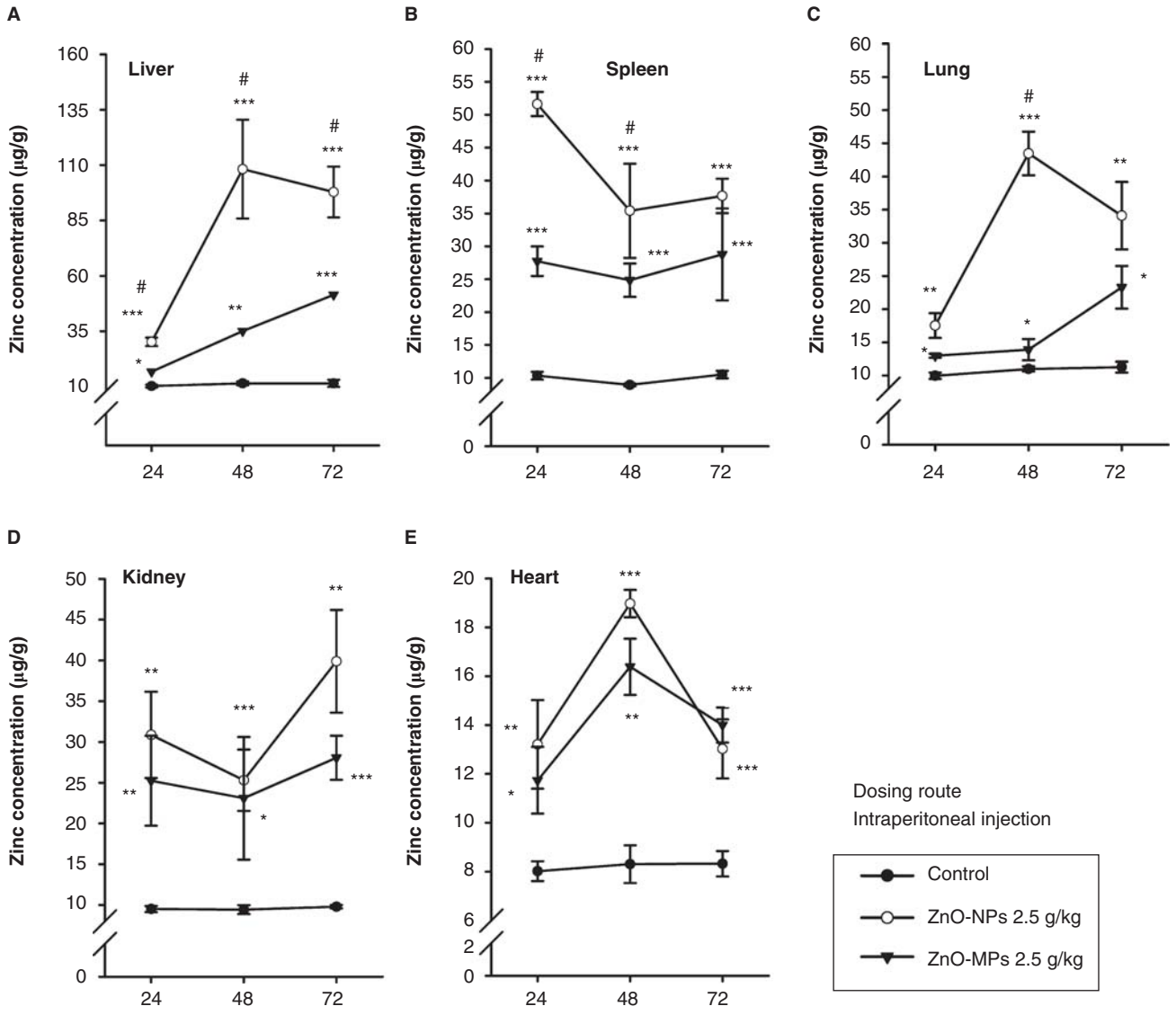

Figure 3. Determination of tissue biodistribution of ZnO-NPs and ZnO-MPs in intraperitoneally injected mice. Isolated tissues from ZnO-NPs (or ZnO-MPs) treated mice (2.5 g/kg b.w.; intraperitoneal injection) were defatted, processed, and analysed by ICP-MS as described in "Materials and methods section. Zinc accumulation was found in liver (A), spleen (B), lung (C), kidney (D), and heart (E). The increased zinc in liver, spleen, and lung of ZnO-NPs treatment showed statistical significance to ZnO-MPs treatment. * $p < 0.05$, ** $p < 0.01$, and *** $p < 0.001$, indicate a statistical difference with the control. # $p < 0.05$, indicates a significant difference with the ZnO-MPs treatment ($N \geq 3$).

among the control, ZnO-NPs treated, and ZnO-MPs treated groups. Figures 6A and 6E show the normal hepatic architecture of the liver of the control group in ZnO-MPs treated mice. In ZnO-NPs treated mice, the histopathological lesions had a mosaic expression, from moderate to severe hepatic swelling and vacuolisation, especially in hepatocytes around the terminal hepatic vein (THV) region (Figures 6C and 6D).

Exposure of ZnO-NPs (or ZnO-MPs) induced superoxide generation and decreased cell viability *in vitro*

Treatment of ZnO-NPs or ZnO-MPs reduced the vitality of cultured cells, including primarily cultured HUVECs, HepG2 (Figures 7A and 7B), A549, and Raw 264.7 (Supplementary Figures 2A and 2B), in a concentration-dependent manner. The calculated lethal concentration, 50% (LC_{50}) of ZnO-NPs and ZnO-MPs were 36.6 and 30.9 µg/mL (HUVECs), 63.6 and 50.1 µg/mL (HepG2), above 200 and 50.2 µg/mL (A549), and 21.2 and 37.7 µg/mL (Raw 264.7). We observed that ZnO-NPs (as well as ZnO-MPs) treatment could induce superoxide generation within 30 min after exposure (Figure 7C), and the induced superoxide could be blocked by ascorbic acid pretreatment (Figure 7D).

Discussion

Absorption of micro- and nano-scaled substances from the site of entry into circulation and various tissues is largely dependent on the portal of entry and particle size (Oberdörster et al. 2005). To assess the hazard characterisation of ZnO-NPs, the absorption has been studied in both orally ingested and intraperitoneally injected manner, and ZnO-MPs were also involved in the study for comparison purposes. A number of studies have indicated that ZnO could release zinc ions in aqueous solution (Massalski et al. 1990). But, the relatively larger surface area of the ZnO-NPs per unit mass when compared with the same mass of ZnO-MPs did

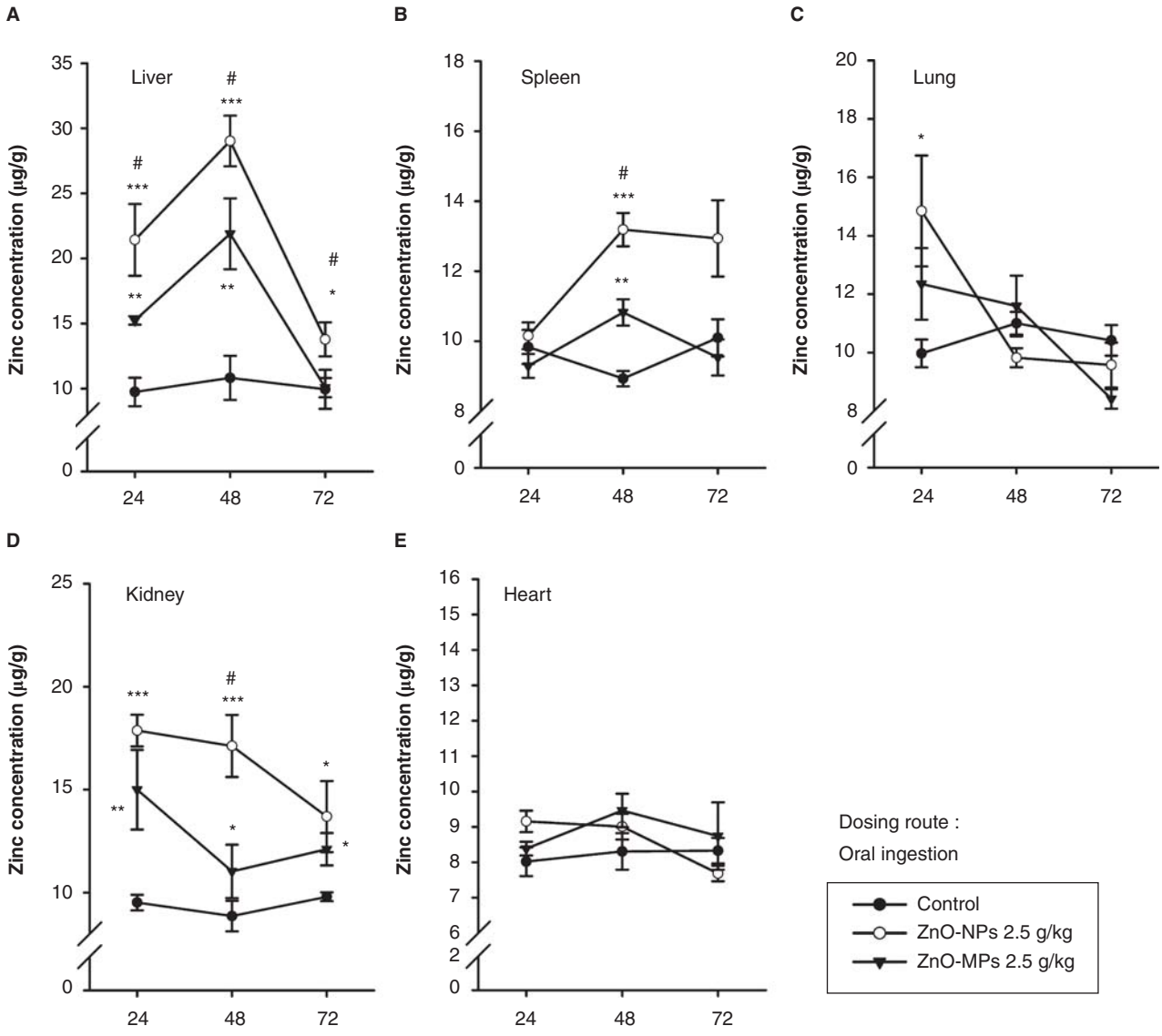

Figure 4. Determination of tissue biodistribution of ZnO-NPs and ZnO-MPs in orally administrated mice. In ZnO-NPs (or ZnO-MPs) treated mice (2.5 g/kg b.w.; oral administration), zinc accumulation was found in the liver (A), spleen (B), lung (C), and kidney (D) but without significant changes in heart (E). Increased zinc in liver, spleen, and kidney of ZnO-NPs treatment showed statistical significance to ZnO-MPs treatment. * $p < 0.05$, ** $p < 0.01$, and *** $p < 0.001$, indicate a statistical difference with the control. # $p < 0.05$, indicates a significant difference with the ZnO-MPs treatment ($N \geq 3$).

not affect the dissociation of zinc ions as suggested in the results of the study for absorption and tissue biodistribution, and proved that this variation was based mainly on the particle size. In this study, both the fed and intraperitoneally injected ZnO-NPs were absorbed into the blood stream where the increase in zinc level could be detected. In both the dosing routes, serum zinc levels peaked within 6 h but gradually declined to the baseline in the orally ingested group, whereas

Table I. Solubility determination of ZnO-NPs and ZnO-MPs.

	Solubility of ZnO-NPs (μg/mL)			Solubility of ZnO-MPs (μg/mL)		
ZnO particles (mg/mL)	pH 2.0	pH 7.0	pH 8.5	pH 2.0	pH 7.0	pH 8.5
0.003	2.23 ± 0.34	0.99 ± 0.07	1.16 ± 0.09	2.35 ± 0.29	1.35 ± 0.29	1.17 ± 0.19
0.03	24.35 ± 2.37	1.18 ± 0.09	1.02 ± 0.11	24.14 ± 5.60	1.09 ± 0.14	1.68 ± 0.11
0.1	78.09 ± 5.30	0.97 ± 0.32	1.00 ± 0.21	88.86 ± 12.04	1.10 ± 0.09	1.52 ± 0.20
1	234.62 ± 23.95	1.37 ± 0.22	1.24 ± 0.23	186.48 ± 13.73	1.77 ± 0.23	1.35 ± 0.24
10	183.71 ± 11.04	1.81 ± 0.34	1.18 ± 0.18	228.55 ± 17.69	0.99 ± 0.15	1.13 ± 0.17
100	319.09 ± 40.49	1.27 ± 0.17	0.96 ± 0.28	254.65 ± 18.11	1.74 ± 0.28	1.67 ± 0.10

Dilutions of ZnO-NPs and ZnO-MPs (0.003, 0.03, 0.1, 1, 10, and 100 mg/mL) were prepared as described in "Nanoparticles" section with the pH value ranging from 2.0 to 8.5. Prepared samples were incubated at 37°C for 2 h followed by centrifuging at 10,000 × *g*. Dissociated zinc in the supernatant was analysed using ICP-MS. For each condition, at least three independent samples were analysed.

The data represented the degree of ZnO-NPs and ZnO-MPs dissociation to zinc ions (solubility; 37°C) in aqueous solution at different pH value, and was presented as mean ± SD from three independent assay ($N = 3$).

No statistical significances existed between ZnO-NPs and ZnO-MPs.

ICP-MS: inductively coupled plasma-mass spectrometry; SD: standard deviation; ZnO-MPs: zinc oxide microparticles; ZnO-NPs: zinc oxide nanoparticles.

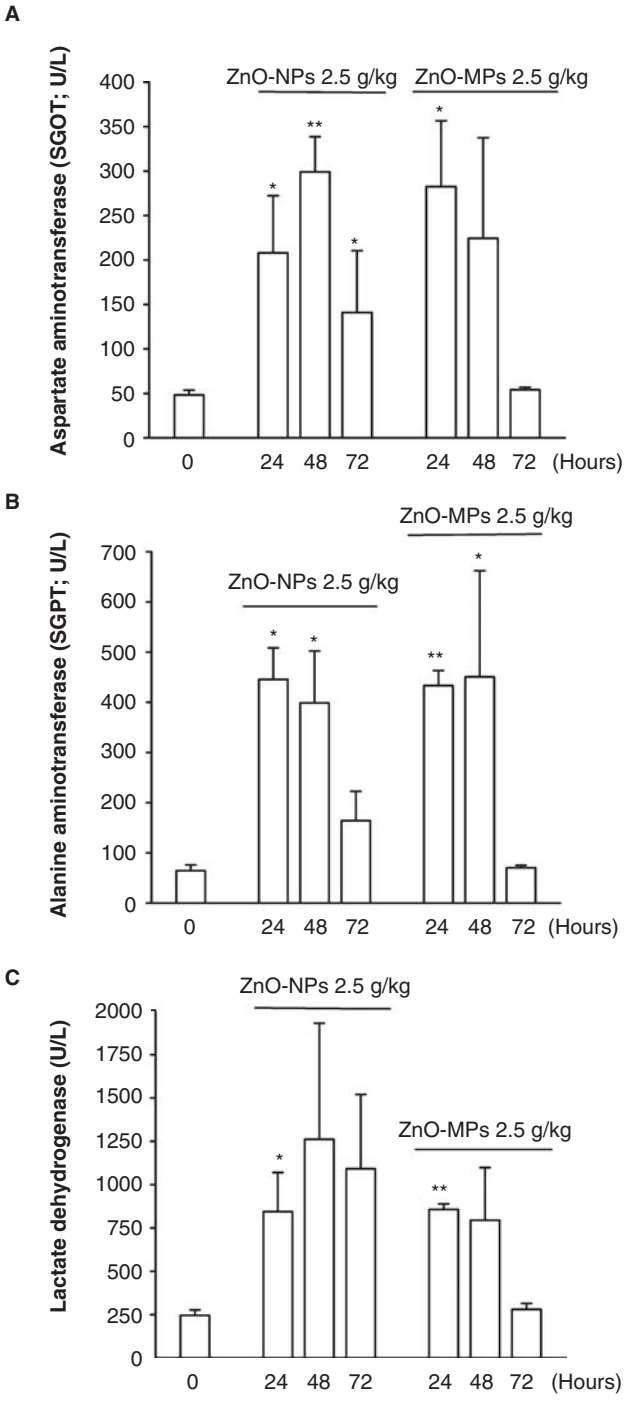

Figure 5. Changes of serum biochemistry biomarkers in ZnO-NPs and ZnO-MPs orally treated mice. The activities of aspartate aminotransferase (AST; also called SGOT) (A), alanine aminotransferase (ALT; also called SGPT) (B), and lactate dehydrogenase (LDH) (C), were augmented in serum biochemistry analysis in ZnO-NPs and ZnO-MPs orally treated mice. * $p < 0.05$, and ** $p < 0.01$, indicate a statistical difference with the control ($N \geq 3$). ZnO-MPs: zinc oxide microparticles; ZnO-NPs: zinc oxide nanoparticles.

the serum zinc levels were sustained in equilibratory level over 72 h in the intraperitoneally injected group. The divergence in clearance revealed that a large proportion of fed ZnO-NPs (or ZnO-MPs) were eliminated directly through fast clearance by defecation. Compared with ZnO-MPs, ZnO-NPs exhibited much higher absorptivity in the orally ingested group, suggesting the size-dependent potential of ZnO particles while absorption after ingestion.

Tissue biodistribution of NPs are quite different between their systemic administration and inhalation. The majority of inhaled NPs stay in the lungs and are primarily associated with alveolar macrophages and capillary endothelial cells (Semmler-Behnke et al. 2008; Oberdörster et al. 2002). However, the internal biodistribution of systemically administered NPs was more towards the liver and spleen (Semmler-Behnke et al. 2008). In this study, both the fed and intraperitoneally injected ZnO-NPs were absorbed and transported via the blood flow, which then reached the liver, spleen, and kidney. The intraperitoneally injected ZnO-NPs could effectively spread to the heart, lung, and

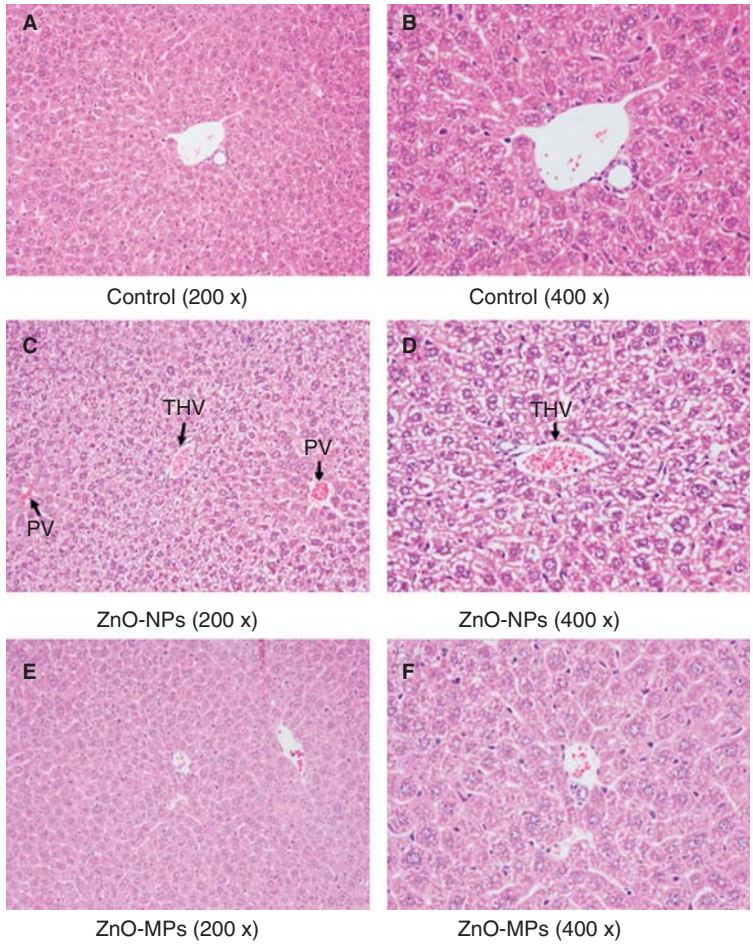

Figure 6. Histopathological lesions of liver were found in ZnO-NPs treated mice. Normal architecture of livers were noted in the control (A. 200×, B. 400×) and ZnO-MPs (E. 200×, F. 400×) treated mice. ZnO-NPs treated mice showed moderate to severe hepatic swelling and vacuolisation (C. 200×, D. 400. The biopsy was prepared from mice sacrificed at 48 h post-gavage. The PV and THV are indicated by the arrows. PV: portal vein; THV: terminal hepatic vein; ZnO-MPs: zinc oxide microparticles; ZnO-NPs: zinc oxide nanoparticles.

testes, where the orally fed particles could not arrive. Interestingly, no change in zinc level was observed in the brain suggesting that the biodistribution could be blocked by blood–brain barrier (BBB). Although the tissue biodistribution pattern of ZnO-NPs and ZnO-MPs were similar, the efficiency of absorption showed diversity, especially in the liver and spleen (also the lung in intraperitoneally injected group and the kidney in orally ingested group). The dosed ZnO-NPs had a better efficiency of absorption and biodistribution than ZnO-MPs.

Liver is the largest depot irrespective of whether ZnO-NPs exposure occurs from intraperitoneal injection or oral ingestion. In liver, NPs could be excreted by bile and bile canaliculi, or removed by the reticuloendothelial system (Johnston et al. 2010). Aside of hepatocytes, the endothelial cells are important scavengers for a number of wastes. NPs sized within 200–500 nm could be internalised by non-phagocytic cells via caveolae-mediated process; internalisation of particles with a diameter of <200 nm was mediated by clathrin-coated pits (Rothen-Rutishauser et al. 2006). After internalisation, the NPs could localise to the mitochondria (Rothen-Rutishauser et al. 2006; Li et al. 2003), endosomes, and lysosomes (Fröhlich et al. 2009) and could activate oxidative stress ultimately leading to genetic damages or mutations in a metabolically active organism. ZnO-NPs have been demonstrated to cause DNA damages (in Comet assay) in Chinese hamster ovary (CHO-K1) cells and human epidermal A431 cells (Dufour et al. 2006; Sharma et al. 2009; Hackenberg et al. 2011). Also, a mutagenic potential have been detected in the presence of metabolic activation (Kumar et al. 2011). On the contrary, either ZnO-NPs or ZnO-MPs showed negative mutagenic responses in this study as well as other earlier cases (Yoshida et al. 2009; Sawai et al. 1998). The contradictions between the results of this study and previous researches may be due to the difference in the sensitivity and reactivity of the analytic approaches. With the use of comet assay, the ZnO-NPs have shown genotoxic effects in all the studies. The high reactivity potential was also seen in other nanoparticles (Karlsson 2010). Therefore, it suggests that in order to obtain a more precise genotoxicity test results, the researchers need to consider the results from not only Comet test but also other methods.

The availability of numerous evidences proved that ZnO particles in environmental pollutants caused generation of ROS, inflammatory responses, and cytotoxicity in the airway epithelium (Heng et al. 2010), microorganisms (Reddy et al. 2007; Raghupathi et al. 2011), mammalian cells (Heng et al.

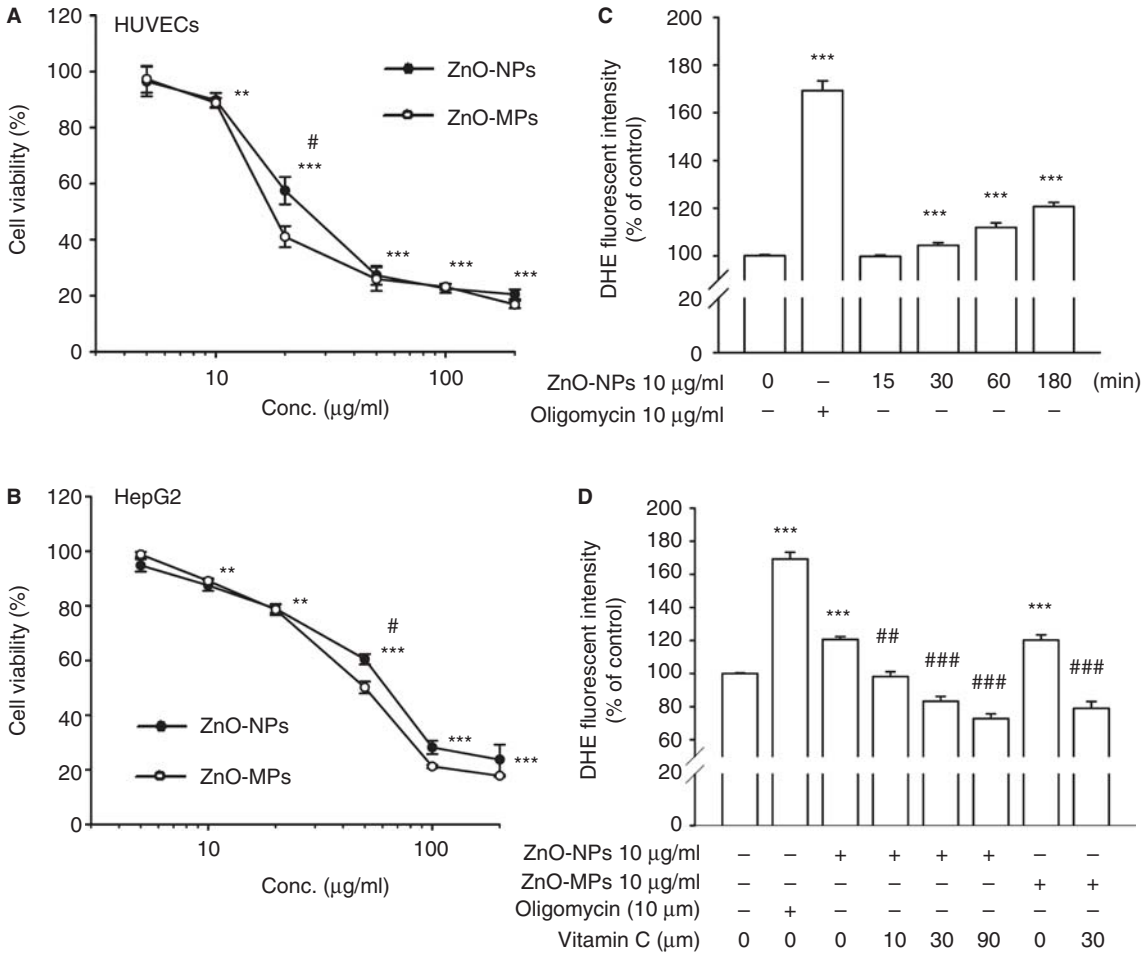

Figure 7. ZnO-NPs and ZnO-MPs exposure induced superoxide generation and decreased cell viability *in vitro*. Cytotoxic effects of ZnO-NPs and ZnO-MPs were evaluated by MTT assay as described in "Materials and methods" section. Both ZnO-NPs and ZnO-MPs caused cell death in concentration-dependent manner (24 h treatment). (A) HUVECs; LC_{50} = 36.6 μg/mL (ZnO-NPs); 30.9 μg/mL (ZnO-MPs), (B) HepG2; LC_{50} = 63.6 μg/mL (ZnO-NPs); 50.1 μg/mL (ZnO-MPs). * $p < 0.05$, ** $p < 0.01$, and *** $p < 0.001$, indicate a statistical difference with the solvent control. # $p < 0.05$, ## $p < 0.01$, and ### $p < 0.001$, indicate a significant difference with the ZnO-MPs treatment. (C) Superoxide generation was measured by DHE as described in "Materials and methods" section. ZnO-NPs (10 μg/mL; 15–180 min incubation) induced superoxide generation in time-dependent manner. Oligomycin was used as positive control. (D) Both ZnO-NPs and ZnO-MPs (10 μg/mL; 180 min treatment) induced superoxide generation could be blocked by ascorbic acid pretreatment. *** $p < 0.001$, indicates a statistical difference with the solvent control. ### $p < 0.01$, indicates a significant difference with the ZnO-treated control. DHE: dihydroethidium; HepG2: hepatocarcinoma cell line; HUVECs: umbilical vein endothelial cells; LC_{50}: lethal concentration, 50%; ZnO-MPs: zinc oxide microparticles; ZnO-NPs: zinc oxide nanoparticles.

2010; Huang et al. 2010), and fish (Zhu et al. 2008). These studies provided ample evidence that ZnO-NPs induced cytotoxicity and this may be partially due to their induction of oxidative stress and oxidative DNA damage. In this study, both ZnO-NPs and ZnO-MPs treatments induced formation of superoxides and resulted in cytotoxicity *in vitro*. The threshold for the occurrence of ZnO-NPs cytotoxicity is 20 μg/mL. This concentration could be detected in both oral and intraperitoneal ZnO-NPs groups of this study. By virtue of increase in serum zinc levels (within 2–6 h) for fed ZnO-NPs, it sufficed to stimulate superoxide generation and resulted in cytotoxic events in the hepatocytes and endothelial cells. Histopathological lesions of the liver suggested the involvement of ROS, in which the damaged hepatocytes were concentrated in the THV regions. Hepatocytes localised around a portal vein (PV) are usually enriched in oxygen and glutathione supplement and are resistant to ROS-induced cytotoxicity. At 48 h post-gavage, the zinc level in the serum and liver returned to the baseline and was in compliance with the decrease in SGOT and SGPT activities. These data suggested that acute toxicity in liver induced by fed ZnO-NPs was dependent on its absorption and clearance.

In this study, both *in vitro* and *in vivo* evidences were gathered to clarify the characteristics of absorption, tissue biodistribution, genotoxicity, and acute toxicity of ZnO-NPs (as well as ZnO-MPs) through orally ingested route. We found that the absorption and tissue targets of ZnO-NPs and ZnO-MPs are similar irrespective of whether the exposure occurs systemically or via oral administration while the proportion of zinc in the liver and spleen varied based on the particle size. Increased zinc levels in the serum and liver corresponded to specific tissue damages. Our data are essential for the safety assessment of clinical usage of ZnO-NPs for the daily supplement of the trace metal zinc, but it also contributes to the health evaluation of workers. Moreover, the inflammatory condition caused by ZnO exposure may in turn alter the sensitivity of cells and tissues to potentially cytotoxic NPs. Further, supportive and extensive

research is needed to explore the complicated toxicity of ZnO-NPs.

Acknowledgments

This study was partly supported by a grant (DOH99-TD-N-111-015) from the Food and Drug Administration, Department of Health, Taiwan.

Declaration of interest

The authors report no conflicts of interest. The authors alone are responsible for the content and writing of the paper.

References

Cheng YW, Lee WW, Li CH, Lee CC, Kang JJ. 2004. Genotoxicity of motorcycle exhaust particles in vivo and in vitro. Toxicol Sci 81:103–111.

Cross SE, Innes B, Roberts MS, Tsuzuki T, Robertson TA, McCormick P. 2007. Human skin penetration of sunscreen nanoparticles: in-vitro assessment of a novel micronized zinc oxide formulation. Skin Pharmacol Physiol 20:148–154.

Dufour EK, Kumaravel T, Nohynek GJ, Kirkland D, Toutain H. 2006. Clastogenicity, photo-clastogenicity or pseudo-photo-clastogenicity: genotoxic effects of zinc oxide in the dark, in pre-irradiated or simultaneously irradiated Chinese hamster ovary cells. Mutat Res 607:215–224.

Fröhlich E, Samberger C, Kueznik T, Absenger M, Roblegg E, Zimmer A, Pieber TR. 2009. Cytotoxicity of nanoparticles independent from oxidative stress. J Toxicol Sci 34:363–375.

Haase H, Overbeck S, Rink L. 2008. Zinc supplementation for the treatment or prevention of disease: current status and future perspectives. Exp Gerontol 43:394–408.

Hackenberg S, Scherzed A, Kessler M, Froelich K, Ginzkey C, Koehler C, et al. 2010. Zinc oxide nanoparticles induce photocatalytic cell death in human head and neck squamous cell carcinoma cell lines in vitro. Int J Oncol 37:1583–1590.

Hackenberg S, Scherzed A, Technau A, Kessler M, Froelich K, Ginzkey C, et al. 2011. Cytotoxic, genotoxic and pro-inflammatory effects of zinc oxide nanoparticles in human nasal mucosa cells in vitro. Toxicol In Vitro 25:657–663.

Heng BC, Zhao X, Xiong S, Ng KW, Boey FY, Loo JS. 2010. Toxicity of zinc oxide (ZnO) nanoparticles on human bronchial epithelial cells (BEAS-2B) is accentuated by oxidative stress. Food Chem Toxicol 48:1762–1766.

Huang CC, Aronstam RS, Chen DR, Huang YW. 2010. Oxidative stress, calcium homeostasis, and altered gene expression in human lung epithelial cells exposed to ZnO nanoparticles. Toxicol In Vitro 24:45–55.

Johnston HJ, Semmler-Behnke M, Brown DM, Kreyling W, Tran L, Stone V. 2010. Evaluating the uptake and intracellular fate of polystyrene nanoparticles by primary and hepatocyte cell lines in vitro. Toxicol Appl Pharmacol 242:66–78.

Karlsson HL. 2010. The comet assay in nanotoxicology research. Anal Bioanal Chem 398:651–666.

Klaine SJ, Alvarez PJ, Batley GE, Fernandes TF, Handy RD, Lyon DY, et al. 2008. Nanomaterials in the environment: behavior, fate, bioavailability, and effects. Environ Toxicol Chem 27:1825–1851.

Kumar A, Pandey AK, Singh SS, Shanker R, Dhawan A. 2011. Cellular uptake and mutagenic potential of metal oxide nanoparticles in bacterial cells. Chemosphere (impress)[Epub ahead of print].

Li N, Sioutas C, Cho A, Schmitz D, Misra C, Sempf J, et al. 2003. Ultrafine particulate pollutants induce oxidative stress and mitochondrial damage. Environ Health Persp 111:455–460.

Liao PL, Cheng YW, Li CH, Lo YL, Kang JJ. 2009. Cholesterol-3-beta, 5-alpha, 6-beta-triol induced PI(3)K-Akt-eNOS-dependent cyclooxygenase-2 expression in endothelial cells. Toxicol Lett 190:172–178.

Maron DM, Ames BN. 1983. Revised methods for the Salmonella mutagenicity test. Mutat Res 113:173–215.

Massalski TB, Murray JL, Bennett LH, Baker H. 1990. Binary alloy phase diagrams. Vol. 3, 2nd ed. OH: ASM, Metals Park. pp. 2938–2939.

Matsumura M, Takasu N, Nagata M, Nakamura K, Kawai M, Yoshino S. 2010. Effect of ultrafine zinc oxide (ZnO) nanoparticles on induction of oral tolerance in mice. J Immunotoxicol 7: 232–237.

Maynard AD, Aitken RJ, Butz T, Colvin V, Donaldson K, Oberdörster G, et al. 2007. Safe handling of nanotechnology. Nature 444:267–269.

Nel A, Xia T, Madler L, Li N. 2006. Toxic potential of materials at the nanolevel. Science 311:622–627.

Oberdörster G, Oberdörster E, Oberdörster J. 2005. Nanotoxicology: an emerging discipline evolving from studies of ultrafine particles. Environ Health Persp 113:823–839.

Oberdörster G, Sharp Z, Atudorei V, Elder A, Gelein R, Lunts A, et al. 2002. Extrapulomnary translocation of ultrafine carbon particles following whole-body inhalation exposure of rats. J Toxicol Environ Health Part A 65:1531–1543.

Pujalté I, Passagne I, Brouillaud B, Tréguer M, Durand E, Ohayon-Courtès C, L'azou B. 2011. Cytotoxicity and oxidative stress induced by different metallic nanoparticles on human kidney cells. Part Fibre Toxicol 3:8–10.

Raghupathi KR, Koodali RT, Manna AC. 2011. Size-dependent bacterial growth inhibition and mechanism of antibacterial activity of zinc oxide nanoparticles. Langmuir 27:4020–4028.

Reddy KM, Feris K, Bell J, Wingett DG, Hanley C, Punnoose A. 2007. Selective toxicity of zinc oxide nanoparticles to prokaryotic and eukaryotic systems. Appl Phys Lett 90:2139021–2139023.

Riehemann K, Schneider SW, Luger TA, Godin B, Ferrari M, Fuchs H. 2009. Nanomedicine – challenge and perspectives. Angew Chem Int Ed Engl 48:872–897.

Rothen-Rutishauser BM, Schurch S, Haenni B, Kapp N, Gehr P. 2006. Interaction of fine particles and nanoparticles with red blood cells visualized with advanced microscopic techniques. Environ Sci Technol 40:4353–4359.

Sawai J, Kojima H, Kano F, Igarashi H, Hashimoto A, Kawada E, et al. 1998. Short communication: Ames assay with Salmonella typhimurium TA102 for mutagenicity and antimutagenicity of metallic oxide powders having antibacterial activities. World J Microbiol Biotechnol 14:773–775.

Semmler-Behnke M, Kreyling WG, Lipka J, Fertsch S, Wenk A, Takenaka S, et al. 2008. Biodistribution of 1.4- and 18-nm gold particles in rats. Small 4:2108–2111.

Sevinc BA, Hanley L. 2010. Antibacterial activity of dental composites containing zinc oxide nanoparticles. J Biomed Mater Res B Appl Biomater 94B:22–31.

Sharma V, Shukla RK, Saxena N, Parmar D, Das M, Dhawan A. 2009. DNA damaging potential of zinc oxide nanoparticles in human epidermal cells. Toxicol Lett 185:211–218.

Stone V, Donaldson K. 2006. Nanotoxicology: signs of stress. Nat Nanotechnol 1:23–24.

Yamaki K, Yoshino S. 2009. Comparison of inhibitory activities of zinc oxide ultrafine and fine particulates on IgE-induced mast cell activation. Biometals 22:1031–1040.

Yoshida R, Kitamura D, Maenosono S. 2009. Mutagenicity of water-soluble ZnO nanoparticles in Ames test. J Toxicol Sci 34: 119–122.

Zhu X, Zhu L, Duan Z, Qi R, Li Y, Lang Y. 2008. Comparative toxicity of several metal oxide nanoparticle aqueous suspensions to Zebrafish (Danio rerio) early developmental stage. J Environ Sci Health A Tox Hazard Subst Environ Eng 43:278–284.

Supplementary material available online

Supplementary Tables I–V.
Supplementary Figures 1, 2.